EXPERIMENTS IN HEAVY ION FUSION BEAM PHYSICS AT LBNL, LLNL, AND THE UNIVERSITY OF MARYLAND

J.W. Kwan, Lawrence Berkeley National Laboratory, Berkeley, CA

Abstract

A heavy ion fusion driver must be capable of accelerating an intense ion beam to GeV beam energies. The final beam pulse current can be as high as a few kA using beam compression in an induction linac. Combining beamlets at low energy may prove to be economical as long as there is no significant emittance growth. Focusing of the final beam pulse from the reactor chamber wall to the target can be enhanced by using a plasma channel to guide the ion beam. Experiments at LBNL on ion sources, injector, the combiner and plasma channel focusing are discussed. One possible way to reduce the cost of a driver is to use an induction recirculator. Experiments at LLNL are exploring this concept by studying the transport and bending of space-charge-dominated ion beams. At the Univ. of Maryland the behavior of space-charge dominated beams is being simulated with low-energy electrons. They studied emittance growth, halo formation and beam pulse compression.

1 INTRODUCTION

The goal of a heavy ion fusion driver is to deliver particle beam power for igniting a fusion target about 5 mm in diameter. To do so, the required beam energy is $\approx$ 5 MJ and the pulse length should be $\approx$ 10 ns in order to achieve a peak power $\approx 10^{15}$ W/cm^2. Furthermore, the energy must be deposited within a short penetration range, e.g. 0.02 to 0.2 g/cm^2 of the target material. For heavy ions with atomic masses $\approx$200, the allowable kinetic energy is $\leq$ 10 GeV [1,2].

Figure 1 is the block diagram of a typical heavy ion fusion driver using induction linacs [3]. Starting with a 2 MeV injector, which may contain up to 100 beams at 1 A per beam, the ions will be accelerated to 100 MeV kinetic energy using electrostatic quadrupole (ESQ) focusing. Above this kinetic energy, the ion velocity is high enough such that magnetic quadrupole focusing becomes more effective. Since an optimal design of the ESQ channel has a smaller bore size and less transportable current than that of the magnetic quadrupole, combining beams at the transition point will minimize the overall cost of a driver. Of course, this is only true if the beam combining process does not significantly degrade the beam quality for the final focusing of beams onto the target.

Assuming an average acceleration rate of 1 MV/m, a 10 GV machine will be 10 km long. One way to reduce the accelerator length is to use lighter ions or high charge state heavy ions which require less beam voltage but more beam current (in the form of more beam channels). For ions of the same q/m ratio, and for a fixed range, the heavier ions are more advantageous because of the higher kinetic energy per nucleon. Another way is to use a
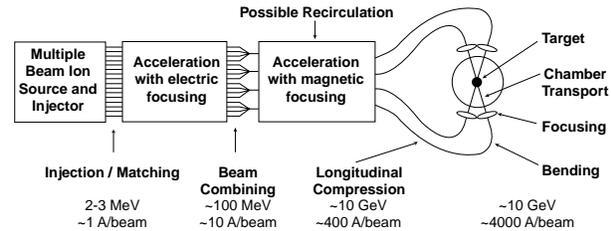

Figure: 1 Block diagram of an HIF induction linac driver.

circular machine so the beams go around many times. Ultimately, the final choice will depend on the physics, the technical difficulties and most importantly the cost.

The increase in ion velocity amplifies the beam current if the beam bunch length remains constant. Furthermore, the acceleration pulse can be arranged to compress the bunch length by giving more kinetic energy to the particles at the rear, therefore producing additional current amplification. In fact, beam compression continues into the drift region beyond the accelerator until the longitudinal space-charge repulsion force eliminates the velocity gradient. While the beam bunch is still in the accelerator, the space-charge repulsion must be balanced by the transverse focusing forces from the quadrupoles and by longitudinal forces due to specially shaped acceleration voltage pulses.

At the final stage of beam focusing, the beam current can be as high as 4 kA/beam. The ability to focus such high current beam onto a 3-mm radius spot size depends greatly on the beam emittance. Some novel ways to relieve the stringent emittance requirement include schemes such as plasma lens and plasma channel beam transport.

Experiments that were designed to address many of these beam physics issues are ongoing at Lawrence Berkeley National Lab (LBNL), Lawrence Livermore National Lab (LLNL) and the University of Maryland (UM). This paper briefly describes some of the more recent experiments and plans.

2 EXPERIMENTS AT LBNL

2.1 Ion Sources and Injectors

Based on beam transport considerations, a 2-MeV injector should provide a beam with a line charge density of approximately 0.25×10^{-6} C/m. The actual beam current will depend on the ion velocity (or equivalently the square root of the charge/mass ratio). For a potassium ion beam, the corresponding beam current is 0.8 A per ion source. For HIF driver applications, the required pulse length at the ion source is about 20×10^{-6} s with a rise time preferably not more than 1×10^{-6} s and a repetition rate of 10 Hz.
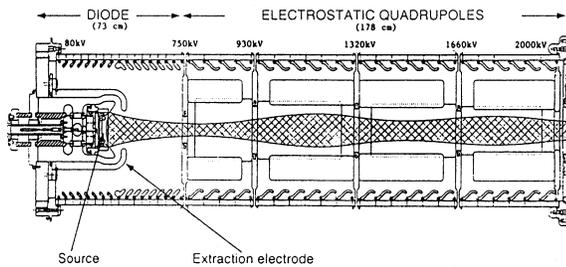
Figure: 2 Schematic Diagram of the 2-MeV ILSE injector.

Figure: 3 Four beams emerging from the combiner.

So far, the surface ionization sources have been selected in most HIF driver designs. The surface ionization type of ion sources can efficiently produce singly charged alkali ions such as Cs^+ and K^+. The major advantages of this type of ion source are the absence of gas flow, excellent beam current control and low emittance (due to low ion temperature and a solid emitter boundary). The main concerns here are the source lifetime, the alkaline vapor delivery system, and the deposition of alkaline vapor onto beam line components. Other types of ion sources should be considered according to their unique properties, for example, a gas source is suitable for generating Hg, Xe, Ar and Ne ions, whereas a metal vapor vacuum arc (MEVVA) source or a laser source would be more appropriate for high charge state ions such as those of Gd and Bi.

Previously, an alumino-silicate ion source has been developed for a 2 MeV injector built for the ILSE/Elise project [4]. A schematic diagram of the ion source and injector is shown in Fig. 2. The injector performance was satisfactory in delivering up to 0.8 A of K^+ ion beam with a normalized edge emittance < 1 π-mm-mrad and it continues to serve as a useful facility for studying HIF beam dynamics including beam profile control and matching the acceptances.

Although this ion source has met the original specifications, the latest conceptual designs for the next HIF research facility calls for an injector with an ion source that has a current density ≥ 15 mA/cm^2 of K^+ (a factor of 4 increase compares to the previous case). A recent experiment has shown that such current density is within the capability of the alumino-silicate ion sources and vapor-fed contact ionizers [5]. The major reason for choosing a high current density, compact size injector is to reduce the overall cost of a fusion driver.

2.2 Beam Combining

The previous MBE-4 experiment on multiple beam transport in induction linacs was successfully completed to show that under optimum conditions the current amplification could be achieved without significant emittance growth [6]. The same facility is now being used for a beam combining experiment.

Fig. 3 shows a layout of 4 beams, each having an elliptical cross-section, arranged in such a way as to be enclosed by a minimum size ellipse. As these beams propagate downstream, they will start to merge into each other forming a single inseparable beam. The merge is not perfect because the empty space within the ellipse
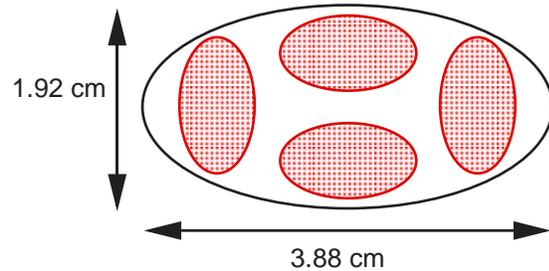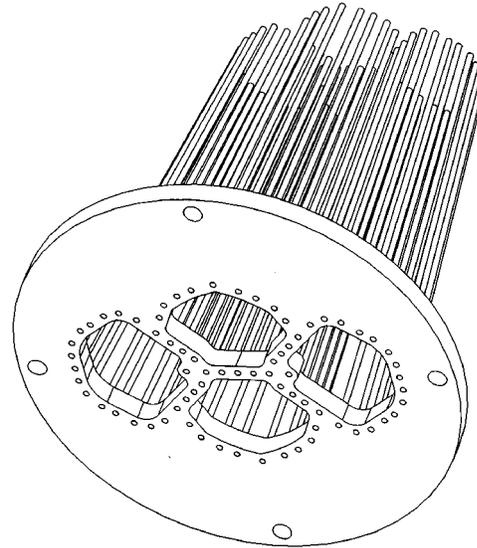

Figure: 4 The wire cage used for combining beams.

boundary is irreversibly blended into the final beam area and the beam emittance.

To minimize the emittance growth, the beams must be brought together independently (i.e. avoid space-charge interaction) until they are closely packed. This is done by using 4 channels of ESQ with a 6° converging angle (w.r.t. center-line) commonly aimed at a merging point where a combined function element called the "wire cage" is located. The device is shown in Fig. 4. It is made of many 1-mm diameter tungsten rods biased at various potential so that the correct Dirichlet boundary condition is established to give both quadrupole field for focusing and dipole field for steering the beams into the proper positions.

The technical difficulties in this experiment are due to the requirements of precise beam alignments and high electric field at the wire cage. Preliminary experimental results [7] are in general agreement with the computer beam simulations.

2.3 Plasma Lens and Channel Transport for Final Focus

The final stage of focusing a very high current heavy ion beam onto the target can be a limiting factor in determining the port size on the chamber wall as well as the number of ports required. Many schemes have been proposed and the major differences among them are the level of space charge and beam current neutralization. While the non-neutralizing lens is only applicable to low current, low charge state ions coupled with a high
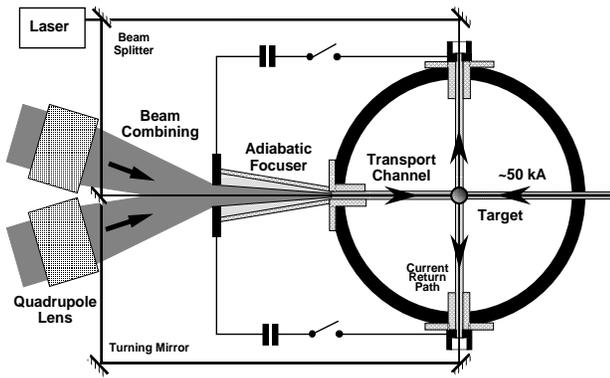
Figure: 5 A proposed scheme for final focus using adiabatic lenses and a discharge channel transport.

0.5 µsec
5.5 kA

1.0 µsec
11.0 kA

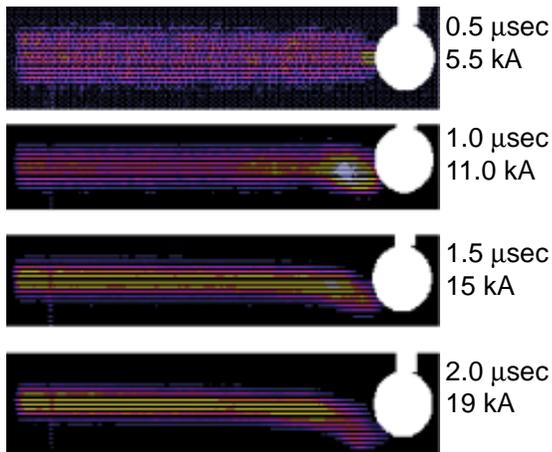1.5 µsec
15 kA

2.0 µsec
19 kA

Figure: 6 Photographs of the plasma channel at various times after the laser trigger.

vacuum in the reactor chamber, neutralizing plasma lens can handle large current (>100 kA), highly stripped ions and are compatible with a moderate chamber pressure. Furthermore, focusing by the plasma lens is achromatic and is insensitive to the beam emittance [8].

Since the beam radius can easily decrease by a factor of more than 3 in passing through the lens, one way to match the focusing properties to this change is by using a tapered discharge tube to adiabatically increase the focusing power along the z-axis. Typically, the entrance radius can be 4-5 times larger than the exit radius. Figure 5 illustrates a final focusing scheme using conventional quadrupole lenses in conjunction with adiabatic lenses and followed by a high current plasma channel to transport the tightly focused ion beam across the chamber radius (≈5 m).

An adiabatic lens experiment was set-up at the 2-MeV injector facility. By passing a small beam through a tapered discharge tube, it was found that the beam current density at the exit changed by a factor of more than 50 between the cases with and without the plasma lens focusing [9].

In a separate experiment, inside a chamber filled with a mixture of nitrogen and benzene, an excimer laser was used to preionize a beam path and then followed by a high voltage discharge [9,10]. The plasma channel produced has a radius of 35 mm, 40 cm long, and up to

19 kA of discharge current. Breakdowns due to surrounding grounded structures was more problematic than hydrodynamic instabilities. In order to simulate the current paths in a reactor chamber (see Fig. 5), a metal ball with the supporting rod as the return current path is inserted at the middle of the experimental chamber to intercept the plasma channel. A series of pictures of the plasma channel at various times after the laser trigger is shown in Fig. 6. The kink at the tip where the electrical current turns a 90° corner is due to the lack of symmetry (purposely arranged in this experiment) from the self-magnetic force. The phenomenon disappeared when the return current was allowed to flow symmetrical on the far side.

3 EXPERIMENTS AT LLNL

A recirculating induction accelerator can reduce the driver cost because it "recycles" the same set of components (≈ 100 laps) for beam acceleration. Similar to an induction linac, the acceleration voltage is provided by induction cores but at a more modest gradient. Nevertheless, the acceleration is rapid enough to avoid the resonant losses of typical circular rf-driven accelerator. Since the ion beams are non-relativistic, the high voltage pulses applied to the induction cores must be continuously adjusted as the beams gain energy. In practice, the dynamic range is about 10-20 times energy gain for each ring, so it will take at least 3 rings to build a 10 GeV driver [11,12].

There are 4 main critical issues in developing the recirculator: (1) power handling, including energy recovery of the dipole magnets, at high repetition rate; (2) beam loss due to inadequate vacuum ($<10^{-10}$ Torr is required); (3) beam dynamics; and (4) feed-back controls.

A small prototype recirculator is being developed at LLNL for experimental studies [13]. Figure 7 shows a schematic diagram of the machine and its designed parameters are tabulated in Table 1. Recently, in a series of experiments, a 65-kV, 1.6-mA K^+ beam was sent through an electrostatic quadrupole matching section,
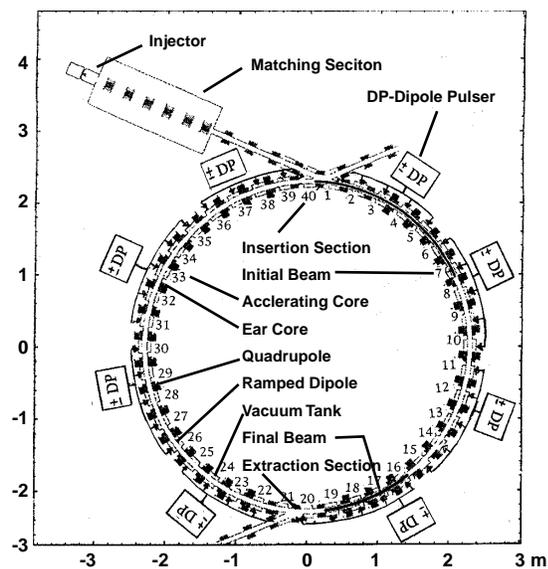

Figure: 7 Schematic diagram of the small recirculator.

Ion species	K$^+$ (mass 39)
Beam energy	80 - 320 keV
Beam current	2 - 8 mA
Pulse duration	4 - 1 µs
Nominal number of laps	15
Circumference	14.4 m
Number of half-lattice period	40
Pipe radius	3.5 cm
Maximum beam radius	1.5 cm
Permanent magnet (at pipe wall)	0.29 T
Undepressed phase advance	78° - 45°
Depressed phase advance	16° - 12°

Table: 1 Design parameters of the small recirculator.

which is followed by a straight transport line of 8 permanent-magnet quadrupole lenses, and then by a 45 degree bend of 5 half-lattice periods. The bending is effected by carefully shaped electric deflector plates.

A special capacitive probe was developed to monitor the beam centroid position [14]. Such non-interceptive beam diagnostics are essential for beam steering corrections in the recirculator. The probe consists of 4 sensing electrodes symmetrically located around the axis, see Fig. 8. The beam centroid x and y positions can be expressed as simple algebraic expressions of the different charges accumulated on the 4 sensors. Excellent agreement was obtained in comparing the measured beam positions against the calculated values.
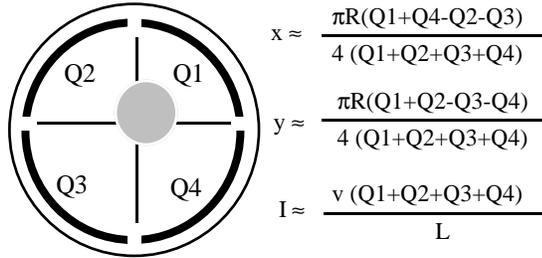
$$x \approx \frac{\pi R (Q1+Q4-Q2-Q3)}{4 (Q1+Q2+Q3+Q4)}$$

$$y \approx \frac{\pi R (Q1+Q2-Q3-Q4)}{4 (Q1+Q2+Q3+Q4)}$$

$$I \approx \frac{v (Q1+Q2+Q3+Q4)}{L}$$

Figure: 8 The capacitive probe as non-interceptive beam diagnostic (R is radius, I is beam current, v is beam velocity, and L is probe length).

4 EXPERIMENTS AT THE UNIVERSITY OF MARYLAND

4.1 Merging Multiple Beams

A low energy electron beam is being used to conduct experiments simulating heavy ion (space-charge dominated) beam transport physics. The facility is a 5 m long periodic solenoid focusing channel system; typical beam parameters are: beam energy 2.5 - 5.0 kV, current 30 - 200 mA, and pulse duration from a few nanoseconds up to a few microseconds. By using a mask with 5 small apertures, arranged in a cross pattern, to produce 5 beamlets, the charge homogenization and emittance growth effects were observed [15]. The experimental set-up is shown in Fig. 9. It was found that the beamlets eventually merged into an almost uniform density single beam. The measured merging distance and the emittance
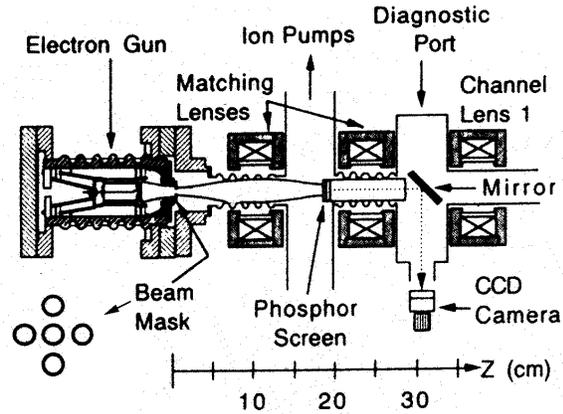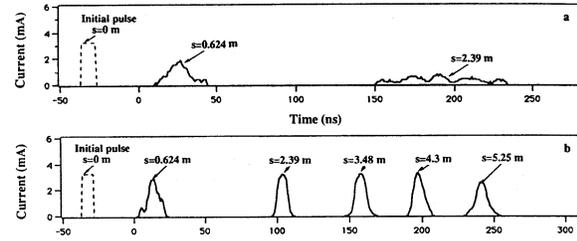
Figure: 9 Schematic of the multi-beam experiment

Figure: 10 Comparison between drift expansion and rectangular pulse restoration: (a) free expansion of a 300 eV, 3.3 mA, 7 ns bunch; (b) beam profiles with restoration.

growth are in good agreement with theoretical prediction as well as computer simulations. The merging distance was near 1/4 beam plasma period and the emittance growth is minimized (a factor ≈3) for rms matched beams. For rms-mismatched beams the halo formation has been observed for the first time in a controlled experiment.

4.2 Space-charge Wave Experiments

The geometry factor g is important in longitudinal beam dynamics because it relates the E_z associated with a perturbation in a beam with the line-charge density variation. By measuring the velocities of the fast and slow (forward and backward in the beam frame) space-charge waves, Wang et al deduced the g factor and confirmed the theoretical model [16] that g=2ln(b/a) where b and a are the pipe radius and the beam radius respectively.

It was also found that a space-charge wave will be partially transmitted and partially reflected at a bunch end [17]. If the beam edge length is much smaller than the perturbation wavelength, there is full reflection and conversely if the ratio is large, then there is no reflection. In addition, by passing the beam through a 1 m long glass tube coated with a layer of indium-tin-oxide on the inside wall (a resistive pipe), the experiment demonstrated the growth of localized slow waves and the decay of fast waves in the long wavelength range [18].

4.3 Longitudinal bunch expansion and Compression

The ends of an initially rectangular line-charge beam bunch usually experience erosion during beam transport.

One way to counter this effect is to apply an "ear" pulse to longitudinally confine the beam particles. An experiment was done by imposing a linear velocity gradient at the beam edge of an eroded beam profile to restore the rectangular shape [19]. Figure 10 shows the beam profiles with and without the restoration.

4.4 Future Development

Figure 11 shows the schematic of a 1.7 m radius electron ring proposed by the Univ. of Maryland. The machine has 36 lattice periods, a 4.9 cm bore radius, a 8.1 G/cm gradient. The quadrupole length is 4.4 cm and has a diameter of 5.3 cm. Injection beam energy is 10 keV and the current is 100 mA. The average beam radius is 1.04 cm with an initial emittance of 10 mm-mrad. Further information on the electron ring development can be found in other papers presented in this meeting [20].
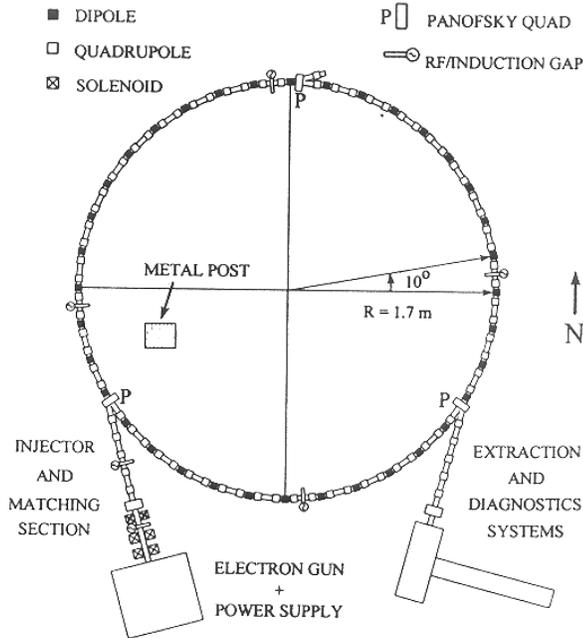

Figure: 11   Layout out of proposed electron ring at the University of Maryland.

5   SUMMARY

The experimental program at LBNL is investigating various means to optimize the accelerator architecture in order to reduce the cost of an induction linac HIF driver. Experiments include high current density ion source and injector, beam combining, and unconventional final focusing. The LLNL approach is to develop the concept of recirculator. In the University of Maryland, electron beams are being used to study many interesting phenomena related to the transport and acceleration of a space-charge-dominated beam bunch. So far, almost all the experiments are scaled down to a much reduced beam energy and current level. In order to make progress towards the construction of a fusion driver, there is an urgent need of a full scale experimental facility for heavy ion fusion research.

REFERENCES

[1] J.D. Lindl, R.L. McCrory and E.M. Campbell, Phys. Today 45, No 9, 32, (1992).

[1] W.J. Hogan, R.O. Bangerter and G.L. Kulcinski, Phys. Today 45, No 9, 42, (1992).

[3] R.O. Bangerter, Proc. of Inter. Symp. on Heavy Ion Inertial Fusion, Frascati, Italy, May 25-28, 1993, Nuovo Cimento 1445 (1993).

[4] S.S. Yu, et al, Proc. of Inter. Symp. on Heavy Ion Inertial Fusion, Princeton, New Jersey, Sept. 6-9, 1995, Fusion Engineering and Design 32-33, 309, (1996).

[5] J.W. Kwan, W.W. Chupp, and S. Eylon, 6W.25, paper in this conf. proceeding.

[6] W.M. Fawley, et al, Phys. Plasmas 4 (3), 880, (1997)

[7] P.A. Seidl, et al, 8V.46, paper in this conf. proceeding.

[8] E. Boggasch, Appl. Phys. Lett. 60, 2475, (1992).

[9] A. Tauschwitz, et al, Proc. of Inter. Symp. on Heavy Ion Inertial Fusion, Princeton, New Jersey, Sept. 6-9, 1995, Fusion Engineering and Design 32-33, 493, (1996).

[10] T.J. Fessenden, and M.C. Vella, HIFAR Note #474, Lawrence Berkeley National Lab, (1997)

[11] J.J. Barnard, et al, Phys. Fluids B: Plasma Phys., 5, 2698, (1993)

[12] A. Friedman, et al, Proc. of Inter. Symp. on Heavy Ion Inertial Fusion, Princeton, New Jersey, Sept. 6-9, 1995, Fusion Engineering and Design 32-33, 235, (1996).

[13] J.J. Barnard, et al, Proc. of Inter. Symp. on Heavy Ion Inertial Fusion, Princeton, New Jersey, Sept. 6-9, 1995, Fusion Engineering and Design 32-33, 235, (1996).

[14] F.J. Deadrick, J.J. Barnard, T.J. Fessenden, J.W. Meridith and J. Rintamaki, Proc. Particle Accel. Conf. Dallas, TX, May 1995, p2557.

[15] M. Reiser, C.R. Chang, D. Kehne, K. Low, and T. Shea, Phys. Rev. Lett. 61, 2993, (1988).

[16] J.G. Wang, H. Suk, D.X. Wang, and M. Reiser, Phys. Rev. Lett. 72, 2029, (1994).

[17] J.G. Wang, D.X. Wang, H. Suk, and M. Reiser, Phys. Rev. Lett. 74, 3153, (1995).

[18] H. Suk, J.G. Wang, Y. Zou, S. Bernal, and M. Reiser, 2V. 28, paper in this conf. proceeding.

[19] D.X. Wang, J.G. Wang, and M. Reiser, Phys. Rev. Lett. 73, 66, (1994).

[20] M. Reiser, et al, 6C.6, 9P.93, 9V.35, 9V. 37, 9V. 38, papers in this conf proceeding.